Computational Statistics and Data Analysis 54 (2010) 2328–2342

Contents lists available at ScienceDirect

Computational Statistics and Data Analysis

journal homepage: www.elsevier.com/locate/csda

# New EWMA control charts for monitoring process dispersion

Longcheen Huwang *, Chun-Jung Huang, Yi-Hua Tina Wang

*Institute of Statistics, National Tsing Hua University, Hsinchu, Taiwan*

ARTICLE INFO

*Article history:*
Received 14 August 2009
Received in revised form 3 March 2010
Accepted 11 March 2010
Available online 25 March 2010

*Keywords:*
Process dispersion
Exponentially weighted moving average
Average run length
ARL-unbiased
In-control
Out-of-control

ABSTRACT

There exist two EWMA-type dispersion charts for monitoring dispersion increases in the literature. One resets the EWMA statistic to zero whenever it is below zero. The other one truncates negative normalized observations to zero in the EWMA statistic. This paper proposes two one-sided EWMA charts for detecting dispersion increases and decreases, respectively, and one two-sided EWMA chart for monitoring dispersion increases or decreases simultaneously. Simulation studies show that the proposed upper-sided EWMA chart performs better than the two existing counterparts for detecting increases in dispersion, and that the proposed lower-sided EWMA chart significantly outperforms the two lower-sided EWMA charts developed similar to their two existing upper-sided EWMA charts for detecting decreases in dispersion. Moreover, the proposed two-sided EWMA chart provides much better sensitivity than the two two-sided EWMA charts generalized from the two existing upper-sided EWMA charts for detecting overall changes in dispersion.



## 1. Introduction

Manufacturing processes can be monitored by using statistical process control (SPC) charts. For example, a Shewhart $\bar{X}$ chart is usually used to monitor the process mean while an $R$ or $S$ chart is adopted to monitor the process dispersion. In most practical applications, it is even more important to monitor changes in process dispersion because an increase of process variance indicates deterioration of the process while a decrease of process variance means an improvement of the process capability. It is meaningless to claim a change of process mean unless it is sure that the process variance is in control.

In addition to the Shewhart $\bar{X}$ chart, the CUSUM (Page, 1954) and EWMA (Roberts, 1959) charts are the two most commonly used charts for monitoring process mean due to their simplicity and good performance. Compared to the Shewhart $\bar{X}$ chart, the advantage of the CUSUM and EWMA charts results from the accumulation of previous and current information for process monitoring. To monitor process dispersion, rational subgroups of samples are collected and the sample range $R$ or variance $S^2$ is then computed for monitoring variability of each subgroup. Riaz (2008) proposed a $Q$ chart based on the interquartile range for monitoring changes in process dispersion. Human et al. (2010) studied the Shewhart-type $S^2$, $S$ and $R$ charts when the mean and variance of the process are estimated from the preliminary data. Similar to the Shewhart $\bar{X}$ chart, the $R$ or $S^2$ chart only uses information of the present subgroup of data and frequently has limited sensitivity to small to moderate changes in process dispersion. Recently more authors had used various CUSUM and EWMA charts for monitoring process dispersion. Jandhyala et al. (2002) studied the null distribution of the generalized likelihood ratio statistic for a step change in the variance of any sequence of independent $\chi^2$ statistics, which can be applied to monitoring process variance. Castagliola (2005) used a three-parameter logarithmic transformation to derive an $S^2$-EWMA chart for monitoring process variance. Knoth (2006) evaluated the performance of CUSUM charts based on $S^2$ for normal processes. Castagliola et al. (2007) introduced a variable sampling interval $S^2$-EWMA chart for monitoring process variance. Machado and Costa

* Corresponding author. Tel.: +886 3 5735385; fax: +886 3 5728318.
*E-mail address:* huwang@stat.nthu.edu.tw (L. Huwang).

0167-9473/$ – see front matter © 2010 Elsevier B.V. All rights reserved.
doi:10.1016/j.csda.2010.03.011

(2008) developed EWMA charts based on the maximum of the two sample variances to monitor the covariance matrix of a bivariate process. Vermaat et al. (2008) proposed EWMA control chart limits for the first- and second-order autoregressive processes. Maravelakis and Castagliola (2009) investigated an EWMA chart for monitoring process standard deviation when parameters of the process are estimated. In addition to the aforementioned papers, there is rich literature related to monitoring process variance. This includes Page (1963), Wortham and Ringer (1971), Hawkins (1981), Sweet (1986), Tuprah and Ncube (1987), Ng and Case (1989), Lowry et al. (1993), Acosta-Mejia and Pignatiello (2000), Sparks (2003), Renolds and Stoumbos (2006), Liu et al. (2007), Chen and Chen (2007), Zhou et al. (2010), and Zhang et al. (2010).

The CUSUM and EWMA charts usually make use of two kinds of statistics for detecting changes in process variance. The first one is the sample variance or the mean squared deviation from the target. Note that either one of the two statistics is skewed to the right. As a consequence, the resulting two-sided CUSUM and EWMA charts for monitoring process variance are frequently ARL-biased procedures. A control chart is ARL-biased if there exists an out-of-control ARL ($ARL_1$) greater than the in-control ARL ($ARL_0$). The second statistic, which the CUSUM and EWMA charts utilize, is usually obtained by transforming the sample variance. The logarithmic transformation of the sample variance, among various transformations, is the most commonly used transformation because the transformed statistic has an approximate normal distribution. A sample of research using $\ln(S^2)$ includes Box et al. (1978, p. 234), Crowder and Hamilton (1992a), Acosta-Mejia et al. (1999), Chen et al. (2001), and Shu and Jiang (2008).

Chang and Gan (1995) compared the performance of the CUSUM charts based on $S^2$ and $\ln(S^2)$. They concluded that both charts have similar performance, but the CUSUM chart based on $S^2$ is slightly better than that based on $\ln(S^2)$ at signaling increases in process variance. Although using $S^2$ in a variance chart gives slightly better efficiency, there may be some advantages of utilizing $\ln(S^2)$ in practice as described below. Note that the distribution of $S^2$ is rightly skewed, and as a result, the two-sided CUSUM or EWMA chart based on $S^2$ would not be symmetrical. In contrast, due to the approximate normality, utilizing $\ln(S^2)$ in the two-sided CUSUM or EWMA chart makes the resulting control limits nearly symmetrical, which would deal with an increase or a decrease of the process variance pretty much the same way. Consequently, unlike using either $S^2$ or mean squared deviation from the target, the two-sided CUSUM or EWMA chart of using $\ln(S^2)$ is nearly ARL-unbiased. It is known that the variance of $\ln(S^2)$ approximately only depends on the sample size, and can be treated as a constant. The stability of the variance of $\ln(S^2)$ results in certain simplicity in establishing control limits for $\ln(S^2)$ as compared to the control charts based on $S^2$. However, both $S^2$ and $\ln(S^2)$ are commonly used in detecting changes in process variance.

Crowder and Hamilton (1992a) were the first to apply the EWMA scheme to the normal approximation of $\ln(S^2/\sigma_0^2)$ for monitoring increases in process variance where $\sigma_0^2$ is the in-control process variance. In order to improve the efficiency for monitoring an increase of the process variance, they reset the EWMA statistic to zero whenever it is below zero. Obviously, the reset of the smaller EWMA statistic to zero can improve the inertia problem of the EWMA statistic and enhance its ability at signaling an increase in the process variance. Based on the similar idea used in Shu et al. (2007) for monitoring process means, Shu and Jiang (2008) proposed truncating $\ln(S^2/\sigma_0^2)$ to its approximate in-control mean whenever it is below the approximate in-control mean. Note that the approximate in-control mean of $\ln(S^2/\sigma_0^2)$ is actually negative (see next section for details) and may remain to be negative when the process variance becomes slightly larger. Thus, when the process is out of control, Crowder and Hamilton's (1992a) approach may cause too much resetting of the EWMA statistic due to the negative value of $\ln(S^2/\sigma_0^2)$. In contrast, Shu and Jiang's (2008) approach only accumulates the positive portion of $\ln(S^2/\sigma_0^2)$ minus its approximate in-control mean at each iteration. Therefore, it could accelerate the detection of an increase in the process variance, in particular when the increase is small. Besides this, Shu and Jiang (2008) claimed that their method being better than Crowder and Hamilton's (1992a) is partially due to the fact that the signal-to-noise (SN) ratio of the statistic they used is higher than that of the statistic $\ln(S^2/\sigma^2)$, which Crowder and Hamilton's (1992a) chart is based on. However, as shown in the next section, it is possible that a charting scheme based on a statistic with a lower SN ratio is more powerful for detecting an increase in the process variance than another scheme based on a different statistic with a higher SN ratio. In fact, a control chart's efficiency for detecting an increase or a decrease in the process variance has no connection with the SN ratio of the statistic used.

In this paper, we propose two one-sided EWMA charts for detecting increases and decreases in process dispersion, respectively. The upper-sided EWMA chart is based on the inverse standard normal distribution function of a chi squared distribution function while the lower-sided EWMA chart is established using a normal approximation to the logarithm of the weighted sum of chi squared random variables. Moreover, we also propose combining the lower-sided and upper-sided EWMA charts as a two-sided EWMA chart for detecting dispersion increases or decreases simultaneously. It is shown that the proposed upper-sided EWMA chart is more effective than the counterparts of Crowder and Hamilton (1992a) and Shu and Jiang (2008) for detecting increases in process dispersion. On the other hand, the proposed lower-sided EWMA chart is significantly more powerful than those developed similar to the upper-sided EWMA charts of Crowder and Hamilton (1992a) and Shu and Jiang (2008) for detecting decreases in process dispersion. Furthermore, the proposed two-sided EWMA chart also outperforms the two-sided EWMA charts generalized from the upper-sided EWMA charts of Crowder and Hamilton (1992a) and Shu and Jiang (2008) for detecting overall changes in process dispersion.

The rest of the paper is organized as follows. The proposed one-sided and two-sided EWMA charts are introduced in the next section. The relationship between the signal-to-noise (SN) ratio of a process change for a control charting scheme and its detection performance is investigated. Then, we compare the performance of the three proposed charts with the

two existing charts in terms of both zero-state and steady-state ARL's. After that, the optimal design of the proposed upper-sided EWMA chart for monitoring dispersion increases and the counterpart of Shu and Jiang (2008) is discussed. Finally some concluding remarks are given.

## 2. The HHW1, HHW2, and HHW-C charts

Suppose that at time $t$ we have a random sample $X_{t1}, X_{t2}, \ldots, X_{tn}$ from a process where each observation follows a normal distribution $N(\mu_t, \sigma_t^2)$. Here, we are only interested in monitoring a change in the process variance. Namely, $\sigma_t^2 = \sigma_0^2$ when $t < \tau$ and $\sigma_t^2 \neq \sigma_0^2$ when $t \geq \tau$ for some time $\tau$ where $\sigma_0^2$ is the in-control process variance. We can assume, without loss of generality, that $\mu_t$ is equal to 0. Let $\delta_t = \sigma_t/\sigma_0$ and $S_t^2 = \sum_{i=1}^{n}(X_{ti} - \bar{X}_t)^2/(n-1)$, $t = 1, 2, \ldots$, be respectively the ratio of process standard deviation and the in-control value and the sample variance based on $X_{t1}, X_{t2}, \ldots, X_{tn}$. Crowder and Hamilton (1992a) proposed the EWMA chart based on

$$Q_t = \max[(1-\lambda)Q_{t-1} + \lambda Y_t, 0], \tag{1}$$

where $0 < \lambda \leq 1$ is a smoothing constant, $Y_t = \ln(S_t^2/\sigma_0^2)$ and $Q_0 = 0$. It is known that $S_t^2/\sigma_0^2$ follows a gamma distribution with shape parameter $\alpha = (n-1)/2$ and scale parameter $\theta = 2\delta_t^2/(n-1)$. Subsequently, $Y_t$ has an approximate normal distribution (see, for example, Lawless (2003)) with mean and variance respectively equal to

$$\mu_Y \approx \ln(\delta_t^2) - \frac{1}{n-1} - \frac{1}{3(n-1)^2} + \frac{2}{15(n-1)^4},$$

and

$$\sigma_Y^2 \approx \frac{2}{n-1} + \frac{2}{(n-1)^2} + \frac{4}{3(n-1)^3} - \frac{16}{15(n-1)^5}. \tag{2}$$

To detect an increase in the process variance, the EWMA in (1) signals an out-of-control if $Q_t$ is greater than

$$h_Q = L_Q\sqrt{\frac{\lambda}{2-\lambda}}\sigma_Y,$$

where $L_Q$ can be determined to achieve a desired $\mathrm{ARL}_0$. Similar to (1), if we are interested in detecting a decrease in the process variance, the EWMA chart can be based on

$$Q_t' = \min[(1-\lambda)Q_{t-1}' + \lambda Y_t, 0],$$

where $Q_0' = 0$ and the chart signals an out-of-control if $Q_t'$ is less than

$$h_Q' = -L_Q'\sqrt{\frac{\lambda}{2-\lambda}}\sigma_Y,$$

where $L_Q'$ can be chosen to achieve a desired $\mathrm{ARL}_0$. For convenience, the charts proposed by Crowder and Hamilton (1992a) will be denoted as the CH charts throughout the rest of this paper.

Define the standardized quantity

$$Z_t = \frac{Y_t - \mu_{Y|\sigma_t=\sigma_0}}{\sigma_Y}, \tag{3}$$

where $\mu_{Y|\sigma_t=\sigma_0}$ is the approximate in-control mean of $Y_t$. Note that the approximate variance of $Y_t$ is a function of $n$ only and thus any changes in $\sigma_t^2$ will only be reflected in the approximate mean $\mu_Y$ of $Y_t$. Denote $Z_t^+ = \max(Z_t, 0)$. If $Z_t$ has an exact standard normal distribution, Barr and Sherrill (1999) showed that $E(Z_t^+) = 1/\sqrt{2\pi}$ and $\sigma_{Z_t^+}^2 = 1/2 - 1/(2\pi)$. As a consequence, Shu and Jiang (2008) proposed an EWMA chart based on

$$W_t = \lambda\left(Z_t^+ - \frac{1}{\sqrt{2\pi}}\right) + (1-\lambda)W_{t-1}, \tag{4}$$

where $W_0 = 0$. The chart declares an out-of-control when $W_t$ exceeds the upper control limit

$$h_N = L_N\sqrt{\frac{\lambda}{2-\lambda}}\sigma_{Z_t^+},$$

where $L_N$ can be chosen to achieve the desired $\mathrm{ARL}_0$. Analogously, if our interest centers on detecting a decrease in the process variance, the EWMA chart can be based on

$$W_t' = \lambda\left(Z_t^- + \frac{1}{\sqrt{2\pi}}\right) + (1-\lambda)W_{t-1}',$$

where $Z_t^- = \min(0,\ Z_t)$ and $W_0' = 0$. Subsequently, the lower control limit of the chart is given by

$$h_N' = -L_N' \sqrt{\frac{\lambda}{2-\lambda}} \sigma_{Z_t^-},$$

where $L_N'$ can be determined to achieve the desired $ARL_0$ and $\sigma_{Z_t^-} = \sigma_{Z_t^+}$. The EWMA charts proposed by Shu and Jiang (2008) will be denoted as the SJ charts in this paper.

Recall that $S_t^2/\sigma_0^2$ has a gamma distribution with shape parameter $\alpha = (n-1)/2$ and scale parameter $\theta = 2\delta_t^2/(n-1)$. It is natural to directly obtain the EWMA statistic

$$V_t = \lambda \frac{S_t^2}{\sigma_0^2} + (1-\lambda) V_{t-1} = \sum_{i=1}^{t} \lambda (1-\lambda)^{t-i} \frac{S_i^2}{\sigma_0^2} + (1-\lambda)^t V_0,$$

where $V_0 = 1$. Due to the independency of $S_i^2$, $i = 1, 2, \ldots, t$, we have, using the two-moment chi squared approximation of Box (1954),

$$V_t - (1-\lambda)^t V_0 = \sum_{i=1}^{t} \lambda (1-\lambda)^{t-i} \frac{S_i^2}{\sigma_0^2} \approx gamma(\beta_1, \beta_2),$$

where

$$\beta_1 = \frac{(n-1)\left[\sum_{i=1}^{t} \lambda(1-\lambda)^{t-i}\right]^2}{2\sum_{i=1}^{t} [\lambda(1-\lambda)^{t-i}]^2} = \frac{(n-1)(2-\lambda)[1-(1-\lambda)^t]^2}{2\lambda[1-(1-\lambda)^{2t}]},$$

and

$$\beta_2 = \frac{2\delta_t^2 \sum_{i=1}^{t} [\lambda(1-\lambda)^{t-i}]^2}{(n-1)\sum_{i=1}^{t} \lambda(1-\lambda)^{t-i}} = \frac{2\lambda[1-(1-\lambda)^{2t}]}{(n-1)(2-\lambda)[1-(1-\lambda)^t]}$$

if $\sigma_t = \cdots = \sigma_1$. Subsequently, taking the logarithm of $V_t - (1-\lambda)^t V_0$, we obtain

$$\ln[V_t - (1-\lambda)^t V_0] \approx N(\mu_R, \sigma_R^2)$$

where

$$\mu_R = \ln(\beta_1 \beta_2) - \frac{1}{2\beta_1} - \frac{1}{12\beta_1^2} + \frac{1}{120\beta_1^4},$$

and

$$\sigma_R^2 = \frac{1}{\beta_1} + \frac{1}{2\beta_1^2} + \frac{1}{6\beta_1^3} - \frac{1}{30\beta_1^5}.$$

The difference between this approach and Shu and Jiang's is that at time $t$, this approach has only employed two approximations, the Box's (1954) two-moment chi squared approximation to obtain a gamma distribution and the normal approximation to the logarithm of the gamma distribution, but Shu and Jiang's approach has used $t$ normal approximations, each approximating the logarithm of a gamma distribution. The distribution of $\ln(S_i^2/\sigma_0^2)$ is actually skewed to the left with a negative mean when the process is in control and may still be negative if the process variance slightly increases. In deriving the EWMA statistics $W_t$ and $W_t'$ for the SJ charts, both statistics involve the addition of $t$ truncated distributions, $Z_t^+$ and $Z_t^-$, $i = 1, 2, \ldots, t$, respectively. Although it may expect a high efficiency of the monitoring statistic $W_t$ for detecting an increase in the process variance, it turns out that the ability of the monitoring statistic $W_t'$ for detecting a decrease in the process variance has been dampened down dramatically. In contrast, the distribution of $V_t - (1-\lambda)^t V_0$, which is a linear combination of $t$ independent chi squared random variables, is approximated by a gamma distribution, and then the logarithm of this gamma distribution is further approximated by a normal distribution. This results in $\ln[V_t - (1-\lambda)^t V_0]$ having a nearly normal distribution. Consequently, the control limits for $\ln[V_t - (1-\lambda)^t V_0]$ is more symmetrical and the ability of detecting an increase or a decrease in the process variance would be roughly the same. On the basis of $\ln[V_t - (1-\lambda)^t V_0]$, we define the standardized monitoring statistic as

$$U_t = \frac{\ln[V_t - (1-\lambda)^t V_0] - \mu_R}{\sigma_R}. \tag{5}$$

Subsequently, the one-sided upper control limit $L_U$ or lower control limit $-L_U$ of $U_t$ can be chosen, respectively, to achieve the desired $ARL_0$. These control charts will be referred to as the HHW1 charts in the paper.

Note that unlike the CH and SJ charts where the monitoring statistics use a constant (independent of $t$) standard deviation to develop the control limits, in the derivation of the control limits for the HHW1 chart, the monitoring statistic $U_t$ equals $\ln[V_t - (1-\lambda)^t V_0] - \mu_R$ divided by the standard deviation $\sigma_R$, which is implicitly a function of $t$. Montgomery (2008) strongly recommended using a variable standard deviation in establishing the control limits for an EWMA chart because it will greatly improve the performance of the control chart in detecting an off-target process immediately after the EWMA is started up. The use of a variable standard deviation turns out to be an advantage of the HHW1 chart over the CH and SJ charts. From the definition of $U_t$ in (5), it can be shown that $U_{t+t_0}$ and $U_t$, $t_0 \geq 1$, have the same distribution if we regard $V_{t_0}$ as the initial value for $V_{t+t_0}$ as is $V_0$ for $V_t$. As a result, the HHW1 chart has the steady-state ARL, denoted by S-ARL, the same as the zero-state ARL, denoted by Z-ARL, at any value of $\sigma$. The Z-ARL is computed assuming a process change occurs at the initial observation of a control chart. The S-ARL is often considered to remove the effect of the initial observation on the chart performance. The S-ARL refers to the ARL computed when the monitoring statistic has arrived steady state before a process change occurred. In contrast, due to the constant standard deviation used in developing the control limits for CH and SJ charts, there may exist notable difference of the Z-ARL and S-ARL at any value of $\sigma$. More discussions about this are included in the section of performance comparison.

An alternative way to detect a change in the process variance is to define the EWMA monitoring statistic in terms of an exact normal transformation of $S_i^2/\sigma_0^2$. Let $F(\cdot)$ be the distribution function of a chi squared random variable with $n-1$ degrees of freedom. It is known that when the process is in control, the statistic $M_t = \Phi^{-1}\{F[(n-1)S_t^2/\sigma_0^2]\}$ has the standard normal distribution, where $\Phi$ is the distribution function of the standard normal distribution. Based on this, the EWMA monitoring statistic is defined by

$$H_t = \lambda M_t + (1-\lambda)H_{t-1},$$

where $H_0 = 0$. It can be shown that $H_t$ has a normal distribution with mean 0 and variance $\lambda[1-(1-\lambda)^{2t}]/(2-\lambda)$ when the process is in control. Since a change in the process variance can result in both changes in the mean and variance of $M_t$, respectively, it is plausible to use the standardized statistic

$$D_t = \frac{H_t}{\sqrt{\frac{\lambda}{2-\lambda}[1-(1-\lambda)^{2t}]}} \tag{6}$$

to monitor the process variance. The two one-sided control charts, which will be denoted as the HHW2 charts in the paper, can be respectively defined by the upper control limit $L_D$ and lower control limit $-L_D$ to achieve the desired $\mathrm{ARL}_0$.

Note that Quesenberry (1995) and Chen et al. (2001) also proposed using the transformation $M_t$ to derive EWMA charts. However, unlike the right hand side of (6) using a variable standard deviation in the denominator, they used constant standard deviations to establish the control limits. As a result, their EWMA charts may have the Z-ARL notably different from the S-ARL due to the effect of initial value.

The CH and SJ charts are developed respectively based on $Y_t = \ln(S_t^2/\sigma_0^2)$ and $Z_t^+$. On the other hand, the HHW1 and HHW2 charts are established based on $S_t^2/\sigma_0^2$ and $M_t$, respectively. Shu and Jiang (2008) compared the SN ratios of $Y_t$ and $Z_t^+$ when the process variance increases, and they concluded that the higher SN ratio of $Z_t^+$ than $Y_t$ may be the reason why the SJ chart has better performance than the CH chart. In the following, we shall compare the SN ratios of $Y_t$, $Z_t^+$, $S_t^2/\sigma_0^2$, and $M_t$ when there is an increase in the process variance from $\sigma_0^2$ to $\sigma^2$. The SN ratio of $Y_t$ is approximated as

$$SN(Y_t) = \frac{Y_t - \mu_{Y|\sigma_t=\sigma_o}}{\sigma_Y} = \frac{\ln(\sigma_t^2/\sigma_0^2)}{\sigma_Y} \equiv \gamma_t.$$

The mean of $Z_t^+$, when $Z_t \sim N(\gamma_t, 1)$, is

$$E(Z_t^+) = \frac{1}{\sqrt{2\pi}} e^{-\gamma_t^2/2} + \gamma_t \Phi(\gamma_t).$$

Consequently, the SN ratio of $Z_t^+$ can be calculated approximately as

$$SN(Z_t^+) = \frac{E(Z_t^+) - E(Z_t^+|\sigma_t=\sigma_0)}{\sigma_{Z_t^+}} = \frac{(e^{-\gamma_t^2/2}-1)/\sqrt{2\pi} + \gamma_t\Phi(\gamma_t)}{\sqrt{1/2 - 1/(2\pi)}}.$$

The SN ratio of $S_t^2/\sigma_0^2$ is

$$SN\left(\frac{S_t^2}{\sigma_0^2}\right) = \frac{E(S_t^2/\sigma_0^2) - E(S_t^2/\sigma_0^2|\sigma_t=\sigma_0)}{\sqrt{Var(S_t^2/\sigma_0^2)}} = \frac{\sigma_t^2/\sigma_0^2 - 1}{\sqrt{2/(n-1)}\sigma_t^2/\sigma_0^2} = \frac{\delta_t^2 - 1}{\sqrt{2/(n-1)}\delta_t^2}.$$

Finally, the SN ratio of $M_t = \Phi^{-1}\{F[(n-1)S_t^2/\sigma_0^2]\}$ is

$$SN(M_t) = \frac{E(M_t) - E(M_t|\sigma_t=\sigma_0)}{\sqrt{Var(M_t)}} = \frac{E(\Phi^{-1}\{F[(n-1)S_t^2/\sigma_0^2]\})}{\sqrt{Var(\Phi^{-1}\{F[(n-1)S_t^2/\sigma_0^2]\})}}.$$

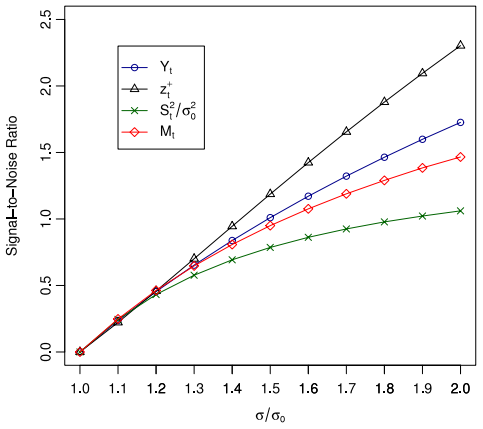


**Fig. 1.** The SN ratios of $Y_t$, $Z_t^+$, $S_t^2/\sigma_0^2$, and $M_t$ when the process variance increases.

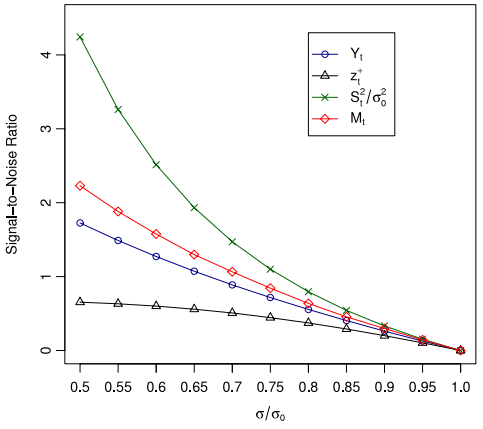


**Fig. 2.** The SN ratios of $Y_t$, $Z_t^+$, $S_t^2/\sigma_0^2$, and $M_t$ when the process variance decreases.

In Fig. 1, we plot the SN ratios of $Y_t$, $Z_t^+$, $S_t^2/\sigma_0^2$, and $M_t$ for $n = 5$ when there is an increase in the process variance. Although $Z_t^+$ has the highest SN ratio among the four competitors, it is shown in the next section that the HHW2 chart is more powerful than the SJ chart for detecting an increase in the process variance. Fig. 2 plots the absolute values of the SN ratios of $Y_t$, $Z_t^+$, $S_t^2/\sigma_0^2$, and $M_t$ for $n = 5$ when there is a decrease in the process variance. It is observed that the CH chart has a higher absolute value of SN ratio than that of the SJ chart despite shown below that the SJ chart gives much better results than the CH chart for detecting a decrease in the process variance. From these two figures, we conclude that the detection performance of a control chart may not have any connection with its SN ratio.

## 3. Performance comparison

In this section, we compare the performance of the CH, SJ, HHW1, and HHW2 charts in terms of ARL. The comparisons are based on the rational subgroup size of $n = 5$. For other different sizes, the results are qualitatively the same and hence are omitted.

As described in Shu and Jiang (2008), both the monitoring statistics $Q_t$ and $W_t$ of the upper-sided CH and SJ charts have a bounded in-control region. Thus discrete Markov chains can be respectively developed to approximate the run-length distributions of the upper-sided CH and SJ charts. On the contrary, the monitoring statistic $U_t(D_t)$ of the upper-sided HHW1(HHW2) chart has an unbounded in-control region due to no resetting being used in deriving $U_t(D_t)$. As a result, it is cumbersome to obtain a discretized Markov chain to approximate the run-length distribution of the upper-sided HHW1(HHW2) chart. Moreover, to express the Z-ARL of the upper-sided HHW1 chart as the solution to an integral equation, one can follow the approach recommended by Crowder and Hamilton (1992b). Let $\delta^2 = \sigma^2/\sigma_0^2$ and $L(\delta^2)$ be the Z-ARL of the upper-sided HHW1 chart starting with $V_0 = \delta^2$. Then, it is easy to show that

$$L(\delta^2) = 1 \cdot P_r(U_1 > L_U) + \int_R \{1 + L[\lambda g + (1-\lambda)\delta^2]\} f(g) \mathrm{d}g,$$

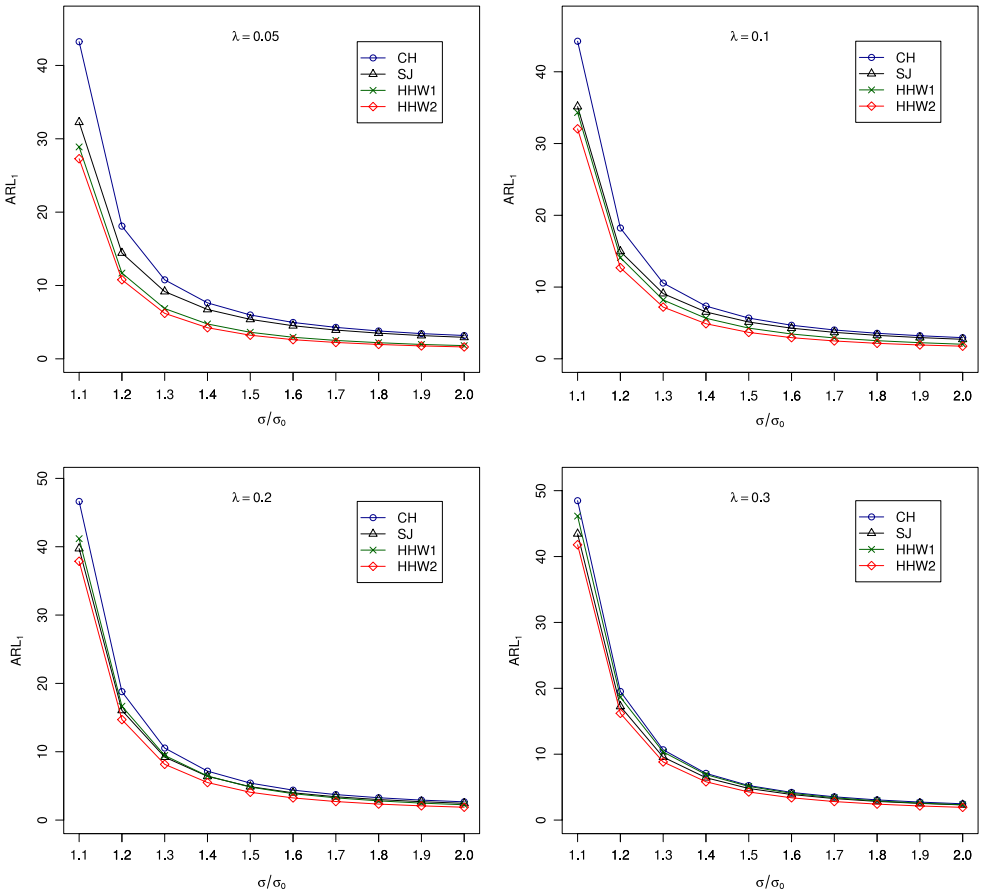


**Fig. 3.** The Z-ARL$_1$'s for the CH, SJ, HHW1, and HHW2 charts when the process variance increases.

where $R = \{g : [ln(\lambda g) - \mu_R]/\sigma_R \leq L_U\}$ and $f(g)$ is the pdf of the gamma random variable $G = S_1^2/\sigma_0^2 = e^{Y_1}$ with shape parameter $(n-1)/2$ and scale parameter $2\delta^2/(n-1)$. Due to the fact that

$$\{U_1 > L_U\} = \left\{\frac{\ln[V_1 - (1-\lambda)\delta^2] - \mu_R}{\sigma_R} > L_U\right\} = \left\{G > \frac{1}{\lambda}e^{\mu_R+\sigma_R L_U}\right\},$$

then

$$\begin{aligned} L(\delta^2) &= P_r\left(G > \frac{1}{\lambda}e^{\mu_R+\sigma_R L_U}\right) + \int_0^{\frac{1}{\lambda}e^{\mu_R+\sigma_R L_U}} \{1 + L[\lambda g + (1-\lambda)\delta^2]\} f(g)\mathrm{d}g \\ &= 1 - F_G\left(\frac{1}{\lambda}e^{\mu_R+\sigma_R L_U}\right) + \int_{-\infty}^{L_U} \{1 + L[e^{\mu_R+\sigma_R h} + (1-\lambda)\delta^2]\} \cdot f\left(\frac{1}{\lambda}e^{\mu_R+\sigma_R h}\right)\frac{\sigma_R}{\lambda}e^{\mu_R+\sigma_R h}\mathrm{d}h, \end{aligned}$$

where $F_G(\cdot)$ is the distribution function of $G$. The Z-ARL of the upper-sided HHW1 chart, $L(\delta^2)$, can be approximately computed using the above integral equation. However, using numerical methods for solving integral equations of this type is difficult because the integral involves integration on the unbounded interval $(-\infty, L_U)$. Due to the aforementioned reasons, in the following we use statistical simulations, which usually produce more accurate results than the Markov chain methodology and the integral equation approach, to compute the Z-ARL's of all control charts being compared. All simulation results in the paper use 200,000 repetitions.

Table 1 tabulates the Z-ARL's for the four competing charts for $n = 5$ and several different values of $\lambda$ ($\leq 0.3$) when the process variance increases. All four charts are set to have an Z-ARL$_0$ of 200. It is evident that among the four control charts, the HHW2 chart has the best performance in detecting an increase in the process variance. For a given value of $\lambda$, the Z-ARL$_1$'s of the HHW2 are uniformly smaller than those of the other three charts. The difference in the Z-ARL$_1$'s among the four charts becomes smaller as $\lambda$ gets closer to 0.3. In Fig. 3, we plot the Z-ARL$_1$'s of the four charts for $\lambda = 0.05, 0.1, 0.2$ and 0.3. It can be observed that the smaller $\lambda$ is, the more prominently the HHW2 chart outperforms the other three charts. Furthermore, for small $\lambda$ values, the superiority of the HHW2 chart is more significantly when the amount of the increase in $\sigma$ is small.

**Table 1**
The zero-state ARL's for the one-sided CH, SJ, HHW1, and HHW2 charts when the process variance increases (( ) = standard error).

| $\lambda = 0.05$ | CH | SJ | HHW1 | HHW2 | $\lambda = 0.1$ | CH | SJ | HHW1 | HHW2 |
|---|---|---|---|---|---|---|---|---|---|
| $\sigma/\sigma_0$ | $L = 1.055$ | 1.568 | 1.828 | 1.872 | $\sigma/\sigma_0$ | $L = 1.303$ | 1.943 | 2.079 | 2.139 |
| 1.0 | 200.33 | 200.75 | 200.92 | 199.57 | 1.0 | 200.02 | 200.36 | 199.51 | 200.35 |
| | (0.44) | (0.45) | (0.47) | (0.49) | | (0.44) | (0.44) | (0.44) | (0.46) |
| 1.1 | 43.24 | 32.26 | 28.89 | 27.28 | 1.1 | 44.26 | 35.15 | 34.32 | 32.05 |
| | (0.09) | (0.06) | (0.06) | (0.06) | | (0.09) | (0.07) | (0.07) | (0.07) |
| 1.2 | 18.09 | 14.43 | 11.69 | 10.78 | 1.2 | 18.23 | 14.96 | 14.10 | 12.69 |
| | (0.03) | (0.02) | (0.02) | (0.02) | | (0.03) | (0.02) | (0.03) | (0.03) |
| 1.3 | 10.77 | 9.17 | 6.85 | 6.20 | 1.3 | 10.56 | 9.09 | 8.20 | 7.21 |
| | (0.02) | (0.01) | (0.01) | (0.01) | | (0.02) | (0.01) | (0.01) | (0.01) |
| 1.4 | 7.63 | 6.73 | 4.75 | 4.24 | 1.4 | 7.35 | 6.53 | 5.65 | 4.89 |
| | (0.01) | (0.01) | (0.01) | (0.01) | | (0.01) | (0.01) | (0.01) | (0.01) |
| 1.5 | 5.98 | 5.38 | 3.62 | 3.22 | 1.5 | 5.68 | 5.13 | 4.28 | 3.68 |
| | (0.01) | (0.01) | (0.01) | (0.01) | | (0.01) | (0.01) | (0.01) | (0.01) |
| 1.6 | 4.96 | 4.51 | 2.94 | 2.61 | 1.6 | 4.68 | 4.27 | 3.46 | 2.95 |
| | (0.01) | (0.00) | (0.00) | (0.00) | | (0.01) | (0.00) | (0.01) | (0.00) |
| 1.7 | 4.29 | 3.92 | 2.51 | 2.23 | 1.7 | 4.02 | 3.69 | 2.91 | 2.49 |
| | (0.00) | (0.00) | (0.00) | (0.00) | | (0.00) | (0.00) | (0.00) | (0.00) |
| 1.8 | 3.80 | 3.50 | 2.20 | 1.96 | 1.8 | 3.56 | 3.27 | 2.53 | 2.16 |
| | (0.00) | (0.00) | (0.00) | (0.00) | | (0.00) | (0.00) | (0.00) | (0.00) |
| 1.9 | 3.44 | 3.17 | 1.96 | 1.76 | 1.9 | 3.22 | 2.96 | 2.25 | 1.93 |
| | (0.00) | (0.00) | (0.00) | (0.00) | | (0.00) | (0.00) | (0.00) | (0.00) |
| 2.0 | 3.18 | 2.93 | 1.80 | 1.62 | 2.0 | 2.95 | 2.72 | 2.03 | 1.76 |
| | (0.00) | (0.00) | (0.00) | (0.00) | | (0.00) | (0.00) | (0.00) | (0.00) |
| $\lambda = 0.2$ | CH | SJ | HHW1 | HHW2 | $\lambda = 0.3$ | CH | SJ | HHW1 | HHW2 |
| $\sigma/\sigma_0$ | $L = 1.513$ | 2.270 | 2.253 | 2.355 | $\sigma/\sigma_0$ | $L = 1.598$ | 2.433 | 2.302 | 2.447 |
| 1.0 | 200.64 | 199.48 | 199.43 | 200.65 | 1.0 | 199.40 | 199.67 | 200.22 | 199.45 |
| | (0.44) | (0.44) | (0.44) | (0.45) | | (0.44) | (0.44) | (0.44) | (0.45) |
| 1.1 | 46.63 | 39.73 | 41.18 | 37.87 | 1.1 | 48.48 | 43.45 | 46.14 | 41.79 |
| | (0.10) | (0.08) | (0.08) | (0.08) | | (0.10) | (0.09) | (0.10) | (0.09) |
| 1.2 | 18.79 | 16.05 | 16.66 | 14.70 | 1.2 | 19.52 | 17.25 | 18.65 | 16.20 |
| | (0.04) | (0.03) | (0.03) | (0.03) | | (0.04) | (0.03) | (0.04) | (0.03) |
| 1.3 | 10.54 | 9.21 | 9.45 | 8.16 | 1.3 | 10.67 | 9.56 | 10.35 | 8.82 |
| | (0.02) | (0.02) | (0.02) | (0.02) | | (0.02) | (0.02) | (0.02) | (0.02) |
| 1.4 | 7.16 | 6.40 | 6.45 | 5.49 | 1.4 | 7.09 | 6.43 | 6.90 | 5.81 |
| | (0.01) | (0.01) | (0.01) | (0.01) | | (0.01) | (0.01) | (0.01) | (0.01) |
| 1.5 | 5.41 | 4.89 | 4.83 | 4.07 | 1.5 | 5.24 | 4.80 | 5.11 | 4.26 |
| | (0.01) | (0.01) | (0.01) | (0.01) | | (0.01) | (0.01) | (0.01) | (0.01) |
| 1.6 | 4.38 | 3.99 | 3.86 | 3.24 | 1.6 | 4.20 | 3.88 | 4.06 | 3.38 |
| | (0.01) | (0.01) | (0.01) | (0.01) | | (0.01) | (0.01) | (0.01) | (0.01) |
| 1.7 | 3.73 | 3.41 | 3.25 | 2.71 | 1.7 | 3.53 | 3.26 | 3.39 | 2.81 |
| | (0.00) | (0.00) | (0.00) | (0.00) | | (0.00) | (0.00) | (0.00) | (0.00) |
| 1.8 | 3.27 | 3.00 | 2.81 | 2.34 | 1.8 | 3.06 | 2.83 | 2.91 | 2.42 |
| | (0.00) | (0.00) | (0.00) | (0.00) | | (0.00) | (0.00) | (0.00) | (0.00) |
| 1.9 | 2.92 | 2.69 | 2.48 | 2.08 | 1.9 | 2.73 | 2.53 | 2.57 | 2.14 |
| | (0.00) | (0.00) | (0.00) | (0.00) | | (0.00) | (0.00) | (0.00) | (0.00) |
| 2.0 | 2.67 | 2.45 | 2.24 | 1.88 | 2.0 | 2.47 | 2.30 | 2.32 | 1.93 |
| | (0.00) | (0.00) | (0.00) | (0.00) | | (0.00) | (0.00) | (0.00) | (0.00) |

Table 2 presents the Z-ARL's for the four competing charts with the same setups as in Table 1 when the process variance decreases. It can be concluded that for a given value of $\lambda$, the Z-ARL$_1$'s of the HHW1 are uniformly smaller than those of the other three charts. The performance improvement of the HHW1 chart is profound especially when the $\lambda$ value is small. Moreover, for small $\lambda$ values, the difference in the Z-ARL$_1$'s between the HHW1 and the other three charts becomes significant when the degree of decrease in $\sigma$ is small. All the aforementioned summary can be easily seen from Fig. 4 which plots the Z-ARL$_1$'s of the four charts for $\lambda = 0.05$, 0.1, 0.2 and 0.3.

In Table 3, the S-ARL's are computed for the four competing charts when there is an increase in the process variance. The S-ARL's are obtained when the monitoring statistics are processed for 25 in-control observations before the run lengths are accumulated to signal. Comparing Table 3 with Table 1, it is observed that for the CH chart, the S-ARL$_1$ is notably smaller than the Z-ARL$_1$ when the process variance increases, and the difference is more significant for the smaller $\lambda$. As for the SJ chart, the S-ARL$_1$ is larger than the Z-ARL$_1$ at an increase in the process variance when $\lambda = 0.05$ and 0.1, but the direction of the discrepancy is not clear and they are not significantly different as $\lambda \geq 0.2$. In contrast, as we have mentioned in the previous section, the HHW1 and HHW2 charts have the same S-ARL$_1$ as the Z-ARL$_1$ when the process variance increases. The

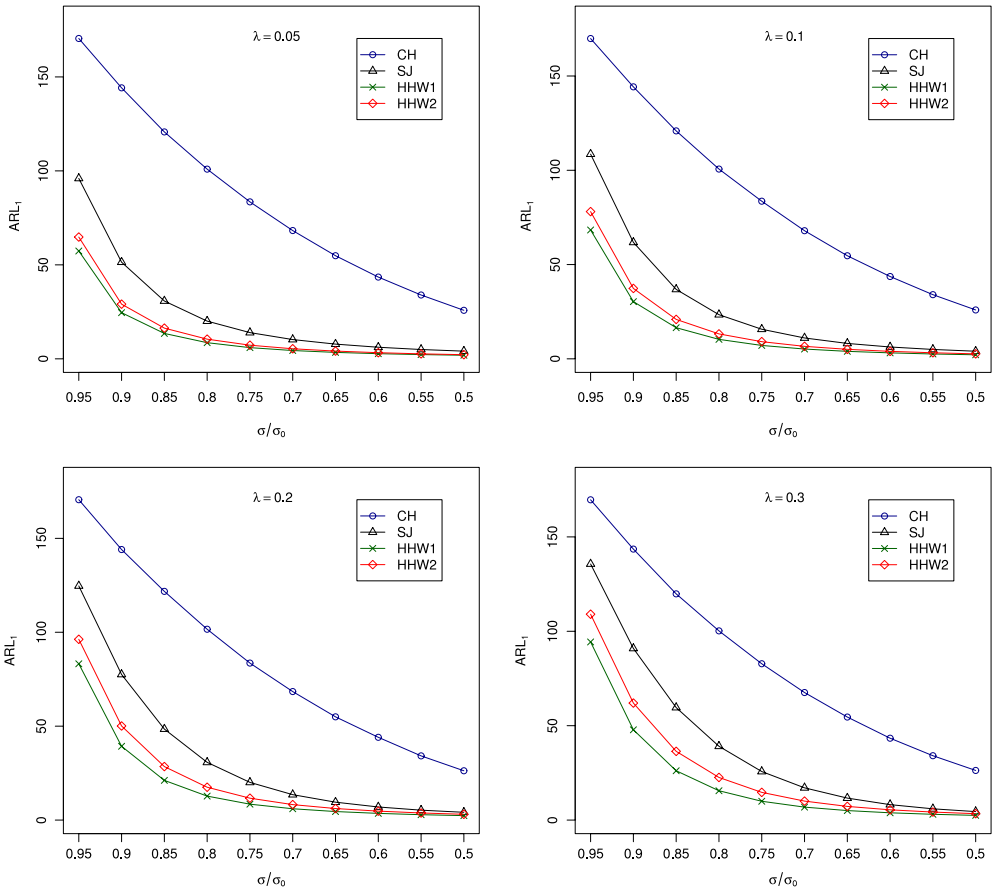


**Fig. 4.** The Z-ARL$_1$'s for the CH, SJ, HHW1, and HHW2 charts when the process variance decreases.

numerical difference between the S-ARL$_1$'s and Z-ARL$_1$'s of the HHW1 or HHW2 chart at an increase in the process variance is purely due to simulation error. Additionally, we have also simulated the S-ARL$_1$'s for the four control charts when there is a decrease in the process variance. Since the conclusions are similar to those in the situation that the process variance increase, they are omitted.

As mentioned earlier, the HHW2 chart gives the best results among the four charts for detecting an increase in the process variance. On the other hand, the HHW1 chart is much more powerful than the other three charts for detecting a decrease in the process variance. Intuitively, instead of using either a two-sided HHW1 chart or a two-sided HHW2 chart, combining a lower-sided HHW1 chart with an upper-sided HHW2 chart may result in better performance for monitoring process variance if we do not know that there is an increase or a decrease in the process variance. In this paper, the two-sided control chart consisting of a lower-sided HHW1 chart and an upper-sided HHW2 chart will be denoted as HHW-C chart.

Table 4 summarizes the Z-ARL's for the two-sided CH, SJ, HHW1, HHW2, and HHW-C charts for $n = 5$ and $\lambda = 0.05$, 0.1, 0.2, 0.3 when the process variance changes. For each of the five two-sided control charts, we use 200,000 Monte Carlo simulations to find the individual $L$ value for each of the two one-sided charts with equal individual Z-ARL$_0$ so that the overall Z-ARL$_0$ of the two-sided chart is approximately equal to 200. According to the results in Table 4, when the process variance decreases, the Z-ARL$_1$'s of the HHW-C chart are practically equivalent to those of the HHW1 chart which has the best performance for detecting a decrease in the process variance. On the other hand, when the process variance increases, the results of the HHW-C chart are not appreciably different from those of the HHW2 chart which outperforms the other charts for detecting an increase in the process variance. Overall, the HHW-C chart is recommended for use when one does not know whether there is an increase or a decrease in the process variance. Furthermore, it is easy to see that the smaller $\lambda$ the better that the HHW-C chart performs.

## 4. Design of the control charts

The design of the control charts studied here involves determining the choice of $\lambda$ and $L$ for a fixed sample size $n$. The design approach recommended by Lucas and Saccucci (1990) and Crowder and Hamilton (1992a) will be followed here. The approach involves the joint choice of $\lambda$ and $L$ that yields a desired Z-ARL$_0$ at the nominal variability ($\sigma = \sigma_0$) and also yields

**Table 2**
The zero-state ARL's for the one-sided CH, SJ, HHW1, and HHW2 charts when the process variance decreases (( ) = standard error).

| $\lambda = 0.05$ | CH | SJ | HHW1 | HHW2 | $\lambda = 0.1$ | CH | SJ | HHW1 | HHW2 |
|---|---|---|---|---|---|---|---|---|---|
| $\sigma/\sigma_0$ | $L = 1.086$ | 2.209 | 1.889 | 1.872 | $\sigma/\sigma_0$ | $L = 1.517$ | 2.843 | 2.145 | 2.140 |
| 1.00 | 199.80 | 199.10 | 200.97 | 199.60 | 1.00 | 199.38 | 200.23 | 200.08 | 199.95 |
| | (0.45) | (0.45) | (0.52) | (0.49) | | (0.45) | (0.44) | (0.49) | (0.46) |
| 0.95 | 170.45 | 95.99 | 57.37 | 64.80 | 0.95 | 169.87 | 108.56 | 68.33 | 78.08 |
| | (0.38) | (0.21) | (0.14) | (0.15) | | (0.38) | (0.23) | (0.16) | (0.17) |
| 0.90 | 144.19 | 51.43 | 24.56 | 29.10 | 0.90 | 144.25 | 61.77 | 30.33 | 37.34 |
| | (0.32) | (0.10) | (0.05) | (0.06) | | (0.32) | (0.13) | (0.07) | (0.08) |
| 0.85 | 120.73 | 30.77 | 13.51 | 16.34 | 0.85 | 120.89 | 36.83 | 16.51 | 20.91 |
| | (0.27) | (0.06) | (0.03) | (0.03) | | (0.27) | (0.07) | (0.03) | (0.04) |
| 0.80 | 100.93 | 20.06 | 8.59 | 10.47 | 0.80 | 100.65 | 23.41 | 10.32 | 13.22 |
| | (0.23) | (0.03) | (0.02) | (0.02) | | (0.22) | (0.04) | (0.02) | (0.02) |
| 0.75 | 83.51 | 13.95 | 5.96 | 7.26 | 0.75 | 83.60 | 15.69 | 7.10 | 9.10 |
| | (0.19) | (0.02) | (0.01) | (0.01) | | (0.19) | (0.03) | (0.01) | (0.01) |
| 0.70 | 68.25 | 10.25 | 4.42 | 5.35 | 0.70 | 67.95 | 11.07 | 5.19 | 6.62 |
| | (0.15) | (0.01) | (0.01) | (0.01) | | (0.15) | (0.02) | (0.01) | (0.01) |
| 0.65 | 54.86 | 7.83 | 3.42 | 4.12 | 0.65 | 54.67 | 8.17 | 3.97 | 5.04 |
| | (0.12) | (0.01) | (0.00) | (0.01) | | (0.12) | (0.01) | (0.01) | (0.01) |
| 0.60 | 43.50 | 6.16 | 2.74 | 3.26 | 0.60 | 43.66 | 6.28 | 3.16 | 3.97 |
| | (0.10) | (0.01) | (0.00) | (0.00) | | (0.10) | (0.01) | (0.00) | (0.00) |
| 0.55 | 33.96 | 4.96 | 2.26 | 2.65 | 0.55 | 34.03 | 4.98 | 2.57 | 3.21 |
| | (0.08) | (0.00) | (0.00) | (0.00) | | (0.08) | (0.01) | (0.00) | (0.00) |
| 0.50 | 25.82 | 4.09 | 1.90 | 2.20 | 0.50 | 25.92 | 4.03 | 2.14 | 2.64 |
| | (0.06) | (0.00) | (0.00) | (0.00) | | (0.06) | (0.00) | (0.00) | (0.00) |
| $\lambda = 0.2$ | CH | SJ | HHW1 | HHW2 | $\lambda = 0.3$ | CH | SJ | HHW1 | HHW2 |
| $\sigma/\sigma_0$ | $L = 2.097$ | 3.525 | 2.346 | 2.354 | $\sigma/\sigma_0$ | $L = 2.500$ | 3.959 | 2.434 | 2.447 |
| 1.00 | 200.53 | 200.64 | 199.80 | 200.24 | 1.00 | 199.74 | 200.88 | 200.07 | 199.36 |
| | (0.45) | (0.44) | (0.47) | (0.45) | | (0.45) | (0.45) | (0.46) | (0.45) |
| 0.95 | 170.58 | 124.67 | 83.21 | 96.26 | 0.95 | 169.65 | 135.65 | 94.35 | 109.05 |
| | (0.38) | (0.27) | (0.19) | (0.21) | | (0.38) | (0.30) | (0.22) | (0.24) |
| 0.90 | 144.05 | 77.53 | 39.29 | 50.10 | 0.90 | 143.54 | 90.92 | 47.82 | 61.98 |
| | (0.32) | (0.17) | (0.09) | (0.11) | | (0.32) | (0.20) | (0.11) | (0.13) |
| 0.85 | 121.77 | 48.45 | 21.13 | 28.48 | 0.85 | 119.83 | 59.59 | 26.13 | 36.41 |
| | (0.27) | (0.10) | (0.04) | (0.06) | | (0.27) | (0.13) | (0.06) | (0.08) |
| 0.80 | 101.61 | 30.73 | 12.76 | 17.49 | 0.80 | 100.22 | 39.10 | 15.54 | 22.58 |
| | (0.23) | (0.06) | (0.02) | (0.03) | | (0.22) | (0.08) | (0.03) | (0.04) |
| 0.75 | 83.59 | 20.07 | 8.47 | 11.65 | 0.75 | 82.81 | 25.71 | 9.96 | 14.68 |
| | (0.19) | (0.04) | (0.01) | (0.02) | | (0.19) | (0.05) | (0.02) | (0.03) |
| 0.70 | 68.43 | 13.53 | 6.02 | 8.23 | 0.70 | 67.56 | 17.08 | 6.86 | 10.05 |
| | (0.15) | (0.02) | (0.01) | (0.01) | | (0.15) | (0.03) | (0.01) | (0.02) |
| 0.65 | 54.97 | 9.53 | 4.54 | 6.14 | 0.65 | 54.57 | 11.64 | 5.03 | 7.24 |
| | (0.12) | (0.01) | (0.01) | (0.01) | | (0.12) | (0.02) | (0.01) | (0.01) |
| 0.60 | 44.07 | 6.97 | 3.56 | 4.76 | 0.60 | 43.36 | 8.17 | 3.85 | 5.43 |
| | (0.10) | (0.01) | (0.00) | (0.01) | | (0.10) | (0.01) | (0.01) | (0.01) |
| 0.55 | 34.18 | 5.27 | 2.86 | 3.78 | 0.55 | 34.09 | 5.96 | 3.06 | 4.24 |
| | (0.08) | (0.01) | (0.00) | (0.00) | | (0.08) | (0.01) | (0.00) | (0.01) |
| 0.50 | 26.25 | 4.14 | 2.37 | 3.08 | 0.50 | 26.29 | 4.49 | 2.49 | 3.38 |
| | (0.06) | (0.00) | (0.00) | (0.00) | | (0.06) | (0.01) | (0.00) | (0.00) |

the smallest Z-ARL$_1$ for a specified change in the process standard deviation. For simplicity, here we only study the design for specific increases in the process standard deviation, and that for specific decreases in the process standard deviation can be similarly dealt with.

Shu and Jiang (2008) used a numerical search method through the Markov chain approximation to find the optimal values of $\lambda$ and $L$ for the SJ charts for the sample sizes of $n = 3, 5, 8, 15$. For a target out-of-control $\sigma(>\sigma_0)$ and a fixed sample size $n$, they found the corresponding values of $L$ with a wide range values of $\lambda$ ($\lambda = 0.01, 0.02, \ldots, 1.0$) to yield the desired Z-ARL$_0$. The pair $(\lambda, L)$ will be considered to be optimal if among all the possible combinations of $\lambda$ and $L$, it produces the smallest Z-ARL$_1$ at the target out-of-control $\sigma$. Following the same numerical search method, we use Monte Carlo simulations to find the optimal parameters for the HHW2 charts for the sample size of $n = 5$ and 15 (the results for $n = 3$ and 8 are omitted). Table 5 compares the results with those of the SJ chart.

As can be seen from Table 5, for a fixed Z-ARL$_0$, unlike the SJ chart whose optimal $\lambda$ value increases as the target out-of-control $\sigma$ becomes larger, the optimal $\lambda$ for the HHW2 chart remains at the value of 0.01 for all the target out-of-control $\sigma$'s considered here. The optimal $\lambda$ remaining at the same value is an advantage of the HHW2 chart which can help one

**Table 3**
The steady-state ARL's for the one-sided CH, SJ, HHW1, and HHW2 charts when the process variance increases (( ) = standard error).

| $\lambda = 0.05$ | CH | SJ | HHW1 | HHW2 | $\lambda = 0.1$ | CH | SJ | HHW1 | HHW2 |
|---|---|---|---|---|---|---|---|---|---|
| $\sigma/\sigma_0$ | $L = 1.055$ | 1.568 | 1.828 | 1.872 | $\sigma/\sigma_0$ | $L = 1.303$ | 1.943 | 2.079 | 2.139 |
| 1.0 | 195.19 | 201.75 | 200.66 | 199.68 | 1.0 | 196.54 | 200.03 | 199.69 | 200.12 |
| | (0.43) | (0.45) | (0.47) | (0.49) | | (0.44) | (0.44) | (0.44) | (0.46) |
| 1.1 | 40.72 | 33.75 | 28.66 | 27.02 | 1.1 | 42.34 | 35.58 | 34.52 | 32.11 |
| | (0.09) | (0.06) | (0.06) | (0.06) | | (0.09) | (0.07) | (0.07) | (0.07) |
| 1.2 | 16.73 | 15.65 | 11.76 | 10.82 | 1.2 | 17.10 | 15.35 | 14.09 | 12.72 |
| | (0.03) | (0.02) | (0.02) | (0.02) | | (0.03) | (0.03) | (0.03) | (0.03) |
| 1.3 | 9.76 | 10.03 | 6.85 | 6.18 | 1.3 | 9.72 | 9.43 | 8.20 | 7.22 |
| | (0.02) | (0.01) | (0.01) | (0.01) | | (0.02) | (0.01) | (0.01) | (0.01) |
| 1.4 | 6.84 | 7.42 | 4.73 | 4.23 | 1.4 | 6.69 | 6.83 | 5.64 | 4.90 |
| | (0.01) | (0.01) | (0.01) | (0.01) | | (0.01) | (0.01) | (0.01) | (0.01) |
| 1.5 | 5.34 | 5.97 | 3.62 | 3.22 | 1.5 | 5.12 | 5.39 | 4.28 | 3.67 |
| | (0.01) | (0.01) | (0.01) | (0.01) | | (0.01) | (0.01) | (0.01) | (0.01) |
| 1.6 | 4.40 | 5.01 | 2.93 | 2.60 | 1.6 | 4.21 | 4.51 | 3.46 | 2.96 |
| | (0.01) | (0.01) | (0.00) | (0.00) | | (0.01) | (0.01) | (0.01) | (0.00) |
| 1.7 | 3.80 | 4.37 | 2.50 | 2.22 | 1.7 | 3.60 | 3.89 | 2.91 | 2.48 |
| | (0.00) | (0.00) | (0.00) | (0.00) | | (0.00) | (0.00) | (0.00) | (0.00) |
| 1.8 | 3.37 | 3.89 | 2.19 | 1.95 | 1.8 | 3.18 | 3.46 | 2.53 | 2.16 |
| | (0.00) | (0.00) | (0.00) | (0.00) | | (0.00) | (0.00) | (0.00) | (0.00) |
| 1.9 | 3.05 | 3.52 | 1.96 | 1.76 | 1.9 | 2.87 | 3.13 | 2.25 | 1.93 |
| | (0.00) | (0.00) | (0.00) | (0.00) | | (0.00) | (0.00) | (0.00) | (0.00) |
| 2.0 | 2.81 | 3.25 | 1.80 | 1.62 | 2.0 | 2.64 | 2.88 | 2.05 | 1.77 |
| | (0.00) | (0.00) | (0.00) | (0.00) | | (0.00) | (0.00) | (0.00) | (0.00) |
| $\lambda = 0.2$ | CH | SJ | HHW1 | HHW2 | $\lambda = 0.3$ | CH | SJ | HHW1 | HHW2 |
| $\sigma/\sigma_0$ | $L = 1.513$ | 2.270 | 2.253 | 2.355 | $\sigma/\sigma_0$ | $L = 1.598$ | 2.433 | 2.302 | 2.447 |
| 1.0 | 197.72 | 198.46 | 199.44 | 200.75 | 1.0 | 198.16 | 199.61 | 200.47 | 199.95 |
| | (0.44) | (0.44) | (0.44) | (0.45) | | (0.44) | (0.44) | (0.44) | (0.45) |
| 1.1 | 45.15 | 39.32 | 41.03 | 37.62 | 1.1 | 47.54 | 43.17 | 46.36 | 41.80 |
| | (0.10) | (0.08) | (0.08) | (0.08) | | (0.10) | (0.09) | (0.10) | (0.09) |
| 1.2 | 17.93 | 15.97 | 16.62 | 14.65 | 1.2 | 18.72 | 17.10 | 18.60 | 16.14 |
| | (0.04) | (0.03) | (0.03) | (0.03) | | (0.04) | (0.03) | (0.04) | (0.03) |
| 1.3 | 9.84 | 9.23 | 9.43 | 8.15 | 1.3 | 10.12 | 9.52 | 10.33 | 8.81 |
| | (0.02) | (0.02) | (0.02) | (0.02) | | (0.02) | (0.02) | (0.02) | (0.02) |
| 1.4 | 6.60 | 6.42 | 6.43 | 5.46 | 1.4 | 6.64 | 6.42 | 6.88 | 5.81 |
| | (0.01) | (0.01) | (0.01) | (0.01) | | (0.01) | (0.01) | (0.01) | (0.01) |
| 1.5 | 4.95 | 4.95 | 4.83 | 4.07 | 1.5 | 4.88 | 4.82 | 5.11 | 4.26 |
| | (0.01) | (0.01) | (0.01) | (0.01) | | (0.01) | (0.01) | (0.01) | (0.01) |
| 1.6 | 4.00 | 4.06 | 3.87 | 3.24 | 1.6 | 3.88 | 3.89 | 4.06 | 3.38 |
| | (0.01) | (0.01) | (0.01) | (0.01) | | (0.01) | (0.01) | (0.01) | (0.01) |
| 1.7 | 3.39 | 3.48 | 3.25 | 2.71 | 1.7 | 3.25 | 3.30 | 3.39 | 2.81 |
| | (0.00) | (0.00) | (0.00) | (0.00) | | (0.00) | (0.00) | (0.00) | (0.00) |
| 1.8 | 2.95 | 3.05 | 2.80 | 2.34 | 1.8 | 2.82 | 2.89 | 2.92 | 2.42 |
| | (0.00) | (0.00) | (0.00) | (0.00) | | (0.00) | (0.00) | (0.00) | (0.00) |
| 1.9 | 2.64 | 2.75 | 2.48 | 2.08 | 1.9 | 2.50 | 2.57 | 2.57 | 2.14 |
| | (0.00) | (0.00) | (0.00) | (0.00) | | (0.00) | (0.00) | (0.00) | (0.00) |
| 2.0 | 2.41 | 2.52 | 2.24 | 1.88 | 2.0 | 2.27 | 2.34 | 2.31 | 1.94 |
| | (0.00) | (0.00) | (0.00) | (0.00) | | (0.00) | (0.00) | (0.00) | (0.00) |

to easily spot the $\lambda$ value for practical use because in reality we do not have any knowledge about the value of the target out-of-control $\sigma$. It is also seen from Table 5 that the minimum Z-ARL$_1$'s for the optimal HHW2 chart are uniformly smaller than those for the optimal SJ chart. Moreover, the performance of both the optimal SJ and HHW2 charts improves as the sample size $n$ becomes larger.

Two points about the optimal parameters $\lambda$ and $L$ discussed above deserve special attention. First, the numerical method used above can only find the approximate optimal values of $\lambda$ and $L$ because the true optimal $\lambda$ may occur at the value different from the prespecified $0.01, \ldots, 0.99, 1$. For example, Table 6 presents the Z-ARL's for the SJ chart based on $(\lambda, L) = (0.001, 0.0345)$, $n = 5$ and Z-ARL$_0$ $= 200$. These Z-ARL$_1$'s are much smaller than those corresponding to the approximate optimal parameters for the SJ chart with $n = 5$ and Z-ARL$_0$ $= 200$ presented in Table 5. Consequently, the approximate optimal parameters in Table 5 are not the true optimal parameters. Secondly, it may be more reasonable to find the optimal value of $\lambda$ from a subinterval away from 0, say $[0.05, 1]$, instead of $(0, 1]$ practically. For a fixed Z-ARL$_0$, smaller $\lambda$ gives smaller Z-ARL$_1$, but, when too small a $\lambda$ is used, the standard deviation of the run-length distribution associated with this Z-ARL$_0$ is usually very large for a control chart. For example, for the HHW2 chart, when $\lambda = 0.01$ the standard deviation

**Table 4**
The zero-state ARL's for the two-sided CH, SJ, HHW1, HHW2, and HHW-C charts when the process variance changes.

| $\lambda = 0.05$ | CH | | SJ | | HHW1 | | HHW2 | | HHW-C | |
|---|---|---|---|---|---|---|---|---|---|---|
| $L_1$ | 1.225 | | 2.812 | | 2.290 | | 2.277 | | 2.302 | |
| $L_2$ | 1.219 | | 1.948 | | 2.233 | | 2.277 | | 2.292 | |
| $\sigma/\sigma_0$ | Z-ARL | s.e. | Z-ARL | s.e. | Z-ARL | s.e. | Z-ARL | s.e. | Z-ARL | s.e. |
| 0.50 | 49.56 | 0.11 | 5.10 | 0.00 | 2.31 | 0.00 | 2.90 | 0.00 | 2.32 | 0.00 |
| 0.55 | 66.21 | 0.15 | 6.25 | 0.01 | 2.79 | 0.00 | 3.55 | 0.00 | 2.80 | 0.00 |
| 0.60 | 85.16 | 0.19 | 7.82 | 0.01 | 3.45 | 0.00 | 4.42 | 0.01 | 3.48 | 0.00 |
| 0.65 | 108.00 | 0.24 | 10.07 | 0.01 | 4.39 | 0.01 | 5.65 | 0.01 | 4.42 | 0.01 |
| 0.70 | 135.06 | 0.30 | 13.46 | 0.02 | 5.80 | 0.01 | 7.48 | 0.01 | 5.84 | 0.01 |
| 0.75 | 165.87 | 0.37 | 18.81 | 0.03 | 8.03 | 0.01 | 10.33 | 0.02 | 8.09 | 0.01 |
| 0.80 | 200.16 | 0.45 | 28.06 | 0.04 | 11.91 | 0.02 | 15.24 | 0.02 | 12.01 | 0.02 |
| 0.85 | 240.82 | 0.54 | 45.86 | 0.08 | 19.53 | 0.04 | 24.74 | 0.04 | 19.66 | 0.04 |
| 0.90 | 280.24 | 0.63 | 83.94 | 0.17 | 38.33 | 0.08 | 47.30 | 0.09 | 38.52 | 0.08 |
| 0.95 | 282.08 | 0.63 | 165.19 | 0.35 | 97.57 | 0.23 | 112.41 | 0.25 | 97.60 | 0.23 |
| 1.00 | 200.69 | 0.44 | 199.89 | 0.44 | 199.66 | 0.49 | 200.64 | 0.48 | 199.98 | 0.51 |
| 1.10 | 57.33 | 0.12 | 45.44 | 0.08 | 43.50 | 0.09 | 41.53 | 0.09 | 41.18 | 0.09 |
| 1.20 | 22.73 | 0.04 | 18.97 | 0.03 | 16.63 | 0.03 | 15.18 | 0.03 | 15.11 | 0.03 |
| 1.30 | 12.93 | 0.02 | 11.59 | 0.01 | 9.43 | 0.02 | 8.34 | 0.02 | 8.33 | 0.02 |
| 1.40 | 8.95 | 0.01 | 8.35 | 0.01 | 6.37 | 0.01 | 5.49 | 0.01 | 5.49 | 0.01 |
| 1.50 | 6.93 | 0.01 | 6.61 | 0.01 | 4.80 | 0.01 | 4.07 | 0.01 | 4.08 | 0.01 |
| 1.60 | 5.72 | 0.01 | 5.52 | 0.01 | 3.85 | 0.01 | 3.23 | 0.01 | 3.23 | 0.01 |
| 1.70 | 4.91 | 0.00 | 4.75 | 0.00 | 3.21 | 0.00 | 2.68 | 0.00 | 2.69 | 0.00 |
| 1.80 | 4.34 | 0.00 | 4.21 | 0.00 | 2.78 | 0.00 | 2.31 | 0.00 | 2.31 | 0.00 |
| 1.90 | 3.91 | 0.00 | 3.80 | 0.00 | 2.45 | 0.00 | 2.05 | 0.00 | 2.05 | 0.00 |
| 2.00 | 3.59 | 0.00 | 3.49 | 0.00 | 2.22 | 0.00 | 1.85 | 0.00 | 1.86 | 0.00 |
| $\lambda = 0.1$ | CH | | SJ | | HHW1 | | HHW2 | | HHW-C | |
| $L_1$ | 1.712 | | 3.434 | | 2.490 | | 2.479 | | 2.497 | |
| $L_2$ | 1.476 | | 2.281 | | 2.413 | | 2.479 | | 2.490 | |
| $\sigma/\sigma_0$ | Z-ARL | s.e. | Z-ARL | s.e. | Z-ARL | s.e. | Z-ARL | s.e. | Z-ARL | s.e. |
| 0.50 | 49.99 | 0.11 | 4.86 | 0.00 | 2.52 | 0.00 | 3.30 | 0.00 | 2.53 | 0.00 |
| 0.55 | 66.42 | 0.15 | 6.09 | 0.01 | 3.08 | 0.00 | 4.06 | 0.00 | 3.09 | 0.00 |
| 0.60 | 85.64 | 0.19 | 7.81 | 0.01 | 3.83 | 0.00 | 5.08 | 0.01 | 3.85 | 0.00 |
| 0.65 | 107.76 | 0.24 | 10.42 | 0.01 | 4.92 | 0.01 | 6.55 | 0.01 | 4.94 | 0.01 |
| 0.70 | 134.63 | 0.30 | 14.55 | 0.02 | 6.55 | 0.01 | 8.73 | 0.01 | 6.58 | 0.01 |
| 0.75 | 164.78 | 0.37 | 21.51 | 0.04 | 9.17 | 0.01 | 12.23 | 0.02 | 9.22 | 0.01 |
| 0.80 | 201.14 | 0.45 | 34.05 | 0.06 | 13.88 | 0.02 | 18.49 | 0.03 | 13.95 | 0.02 |
| 0.85 | 240.43 | 0.54 | 57.97 | 0.12 | 23.55 | 0.05 | 31.14 | 0.06 | 23.70 | 0.05 |
| 0.90 | 277.76 | 0.62 | 105.29 | 0.22 | 47.78 | 0.10 | 60.74 | 0.13 | 48.01 | 0.10 |
| 0.95 | 276.23 | 0.62 | 186.78 | 0.41 | 116.48 | 0.27 | 134.52 | 0.30 | 117.17 | 0.27 |
| 1.00 | 199.59 | 0.44 | 200.37 | 0.44 | 199.77 | 0.46 | 199.72 | 0.46 | 200.02 | 0.47 |
| 1.10 | 59.91 | 0.12 | 50.04 | 0.10 | 51.62 | 0.11 | 48.06 | 0.10 | 48.08 | 0.11 |
| 1.20 | 23.25 | 0.04 | 19.37 | 0.03 | 19.17 | 0.03 | 17.20 | 0.03 | 17.17 | 0.03 |
| 1.30 | 12.83 | 0.02 | 11.22 | 0.02 | 10.71 | 0.02 | 9.31 | 0.02 | 9.30 | 0.02 |
| 1.40 | 8.65 | 0.01 | 7.84 | 0.01 | 7.19 | 0.01 | 6.11 | 0.01 | 6.12 | 0.01 |
| 1.50 | 6.56 | 0.01 | 6.06 | 0.01 | 5.37 | 0.01 | 4.47 | 0.01 | 4.48 | 0.01 |
| 1.60 | 5.35 | 0.01 | 4.99 | 0.01 | 4.28 | 0.01 | 3.51 | 0.01 | 3.52 | 0.01 |
| 1.70 | 4.56 | 0.00 | 4.29 | 0.00 | 3.58 | 0.00 | 2.92 | 0.00 | 2.92 | 0.00 |
| 1.80 | 4.00 | 0.00 | 3.78 | 0.00 | 3.08 | 0.00 | 2.50 | 0.00 | 2.50 | 0.00 |
| 1.90 | 3.60 | 0.00 | 3.41 | 0.00 | 2.71 | 0.00 | 2.20 | 0.00 | 2.20 | 0.00 |
| 2.00 | 3.29 | 0.00 | 3.12 | 0.00 | 2.43 | 0.00 | 1.98 | 0.00 | 1.98 | 0.00 |
| $\lambda = 0.2$ | CH | | SJ | | HHW1 | | HHW2 | | HHW-C | |
| $L_1$ | 2.362 | | 4.134 | | 2.649 | | 2.644 | | 2.654 | |
| $L_2$ | 1.680 | | 2.576 | | 2.526 | | 2.644 | | 2.651 | |
| $\sigma/\sigma_0$ | Z-ARL | s.e. | Z-ARL | s.e. | Z-ARL | s.e. | Z-ARL | s.e. | Z-ARL | s.e. |
| 0.50 | 50.47 | 0.11 | 5.03 | 0.01 | 2.74 | 0.00 | 3.74 | 0.00 | 2.75 | 0.00 |
| 0.55 | 66.63 | 0.15 | 6.59 | 0.01 | 3.36 | 0.00 | 4.66 | 0.01 | 3.37 | 0.00 |
| 0.60 | 85.76 | 0.19 | 9.00 | 0.01 | 4.26 | 0.01 | 5.96 | 0.01 | 4.27 | 0.01 |
| 0.65 | 107.54 | 0.24 | 12.80 | 0.02 | 5.55 | 0.01 | 7.87 | 0.01 | 5.57 | 0.01 |
| 0.70 | 133.49 | 0.30 | 19.13 | 0.03 | 7.61 | 0.01 | 10.93 | 0.02 | 7.64 | 0.01 |
| 0.75 | 165.20 | 0.37 | 30.18 | 0.06 | 11.11 | 0.02 | 16.17 | 0.03 | 11.16 | 0.02 |

(*continued on next page*)

Table 4 (*continued*)

| | | | | | | | | | |
|---|---|---|---|---|---|---|---|---|---|
| 0.80 | 200.12 | 0.45 | 49.32 | 0.10 | 17.80 | 0.03 | 25.83 | 0.05 | 17.90 | 0.03 |
| 0.85 | 239.03 | 0.54 | 82.89 | 0.18 | 31.89 | 0.07 | 45.09 | 0.09 | 32.10 | 0.07 |
| 0.90 | 273.64 | 0.61 | 139.87 | 0.30 | 65.23 | 0.15 | 86.24 | 0.19 | 65.78 | 0.15 |
| 0.95 | 270.76 | 0.60 | 208.95 | 0.46 | 139.60 | 0.32 | 163.63 | 0.36 | 141.57 | 0.33 |
| 1.00 | 199.49 | 0.44 | 200.19 | 0.44 | 199.41 | 0.46 | 199.73 | 0.45 | 199.85 | 0.46 |
| 1.10 | 64.17 | 0.14 | 57.76 | 0.12 | 63.30 | 0.13 | 56.94 | 0.12 | 57.30 | 0.13 |
| 1.20 | 24.62 | 0.05 | 21.31 | 0.04 | 22.84 | 0.04 | 19.92 | 0.04 | 19.90 | 0.04 |
| 1.30 | 13.04 | 0.02 | 11.50 | 0.02 | 12.21 | 0.02 | 10.39 | 0.02 | 10.38 | 0.02 |
| 1.40 | 8.47 | 0.01 | 7.64 | 0.01 | 8.00 | 0.01 | 6.68 | 0.01 | 6.68 | 0.01 |
| 1.50 | 6.25 | 0.01 | 5.72 | 0.01 | 5.87 | 0.01 | 4.83 | 0.01 | 4.83 | 0.01 |
| 1.60 | 4.99 | 0.01 | 4.61 | 0.01 | 4.63 | 0.01 | 3.78 | 0.01 | 3.78 | 0.01 |
| 1.70 | 4.21 | 0.01 | 3.91 | 0.00 | 3.86 | 0.01 | 3.11 | 0.00 | 3.12 | 0.00 |
| 1.80 | 3.66 | 0.00 | 3.41 | 0.00 | 3.30 | 0.00 | 2.66 | 0.00 | 2.66 | 0.00 |
| 1.90 | 3.26 | 0.00 | 3.05 | 0.00 | 2.90 | 0.00 | 2.33 | 0.00 | 2.33 | 0.00 |
| 2.00 | 2.96 | 0.00 | 2.77 | 0.00 | 2.60 | 0.00 | 2.09 | 0.00 | 2.09 | 0.00 |
| $\lambda = 0.3$ | CH | | SJ | | HHW1 | | HHW2 | | HHW-C | |
| $L_1$ | 2.818 | | 4.599 | | 2.718 | | 2.718 | | 2.722 | |
| $L_2$ | 1.758 | | 2.716 | | 2.540 | | 2.718 | | 2.723 | |
| $\sigma/\sigma_0$ | Z-ARL | s.e. | Z-ARL | s.e. | Z-ARL | s.e. | Z-ARL | s.e. | Z-ARL | s.e. |
| 0.50 | 50.89 | 0.11 | 5.70 | 0.01 | 2.88 | 0.00 | 4.14 | 0.00 | 2.89 | 0.00 |
| 0.55 | 66.23 | 0.15 | 7.86 | 0.01 | 3.60 | 0.00 | 5.28 | 0.01 | 3.60 | 0.00 |
| 0.60 | 85.30 | 0.19 | 11.36 | 0.02 | 4.65 | 0.01 | 7.01 | 0.01 | 4.66 | 0.01 |
| 0.65 | 107.05 | 0.24 | 17.07 | 0.03 | 6.26 | 0.01 | 9.70 | 0.02 | 6.27 | 0.01 |
| 0.70 | 133.04 | 0.30 | 26.54 | 0.05 | 8.93 | 0.02 | 14.13 | 0.02 | 8.96 | 0.02 |
| 0.75 | 164.19 | 0.37 | 42.31 | 0.09 | 13.66 | 0.03 | 21.84 | 0.04 | 13.72 | 0.03 |
| 0.80 | 198.08 | 0.44 | 67.52 | 0.15 | 22.78 | 0.05 | 35.66 | 0.07 | 22.90 | 0.05 |
| 0.85 | 236.86 | 0.53 | 107.97 | 0.24 | 41.44 | 0.09 | 61.91 | 0.13 | 41.71 | 0.09 |
| 0.90 | 269.89 | 0.60 | 167.04 | 0.37 | 81.15 | 0.18 | 110.38 | 0.24 | 81.96 | 0.19 |
| 0.95 | 265.65 | 0.59 | 222.16 | 0.49 | 155.61 | 0.36 | 183.58 | 0.41 | 158.53 | 0.36 |
| 1.00 | 200.41 | 0.45 | 200.04 | 0.44 | 199.52 | 0.45 | 200.30 | 0.45 | 199.90 | 0.46 |
| 1.10 | 68.48 | 0.15 | 63.90 | 0.14 | 72.52 | 0.16 | 64.10 | 0.14 | 64.90 | 0.14 |
| 1.20 | 26.29 | 0.05 | 23.45 | 0.05 | 26.26 | 0.05 | 22.49 | 0.05 | 22.51 | 0.05 |
| 1.30 | 13.53 | 0.03 | 12.14 | 0.02 | 13.54 | 0.02 | 11.39 | 0.02 | 11.39 | 0.02 |
| 1.40 | 8.53 | 0.01 | 7.76 | 0.01 | 8.58 | 0.01 | 7.10 | 0.01 | 7.10 | 0.01 |
| 1.50 | 6.18 | 0.01 | 5.68 | 0.01 | 6.21 | 0.01 | 5.09 | 0.01 | 5.09 | 0.01 |
| 1.60 | 4.82 | 0.01 | 4.47 | 0.01 | 4.83 | 0.01 | 3.93 | 0.01 | 3.93 | 0.01 |
| 1.70 | 4.01 | 0.01 | 3.74 | 0.00 | 3.98 | 0.01 | 3.22 | 0.01 | 3.22 | 0.01 |
| 1.80 | 3.46 | 0.00 | 3.23 | 0.00 | 3.40 | 0.00 | 2.74 | 0.00 | 2.74 | 0.00 |
| 1.90 | 3.05 | 0.00 | 2.85 | 0.00 | 2.96 | 0.00 | 2.38 | 0.00 | 2.39 | 0.00 |
| 2.00 | 2.74 | 0.00 | 2.57 | 0.00 | 2.64 | 0.00 | 2.14 | 0.00 | 2.14 | 0.00 |

of the run-length distribution associated with Z-ARL$_0$ = 200 equals 315.5, which is much larger than the counterpart of the value 219.1 when $\lambda = 0.05$. Large variability of run-length distribution at small value of $\lambda$ usually prevents the practitioner from choosing it as the smoothing constant to use in practice.

## 5. Concluding remarks

In this paper, we have proposed and studied two control charting schemes, HHW1 and HHW2 charts, for monitoring decreases and increases in process variability, respectively. Based on the simulation studies, the HHW2 chart performs better than the CH, SJ and HHW1 charts for detecting increases in process variability. The HHW1 chart, on the other hand, significantly outperforms the CH, SJ and HHW2 charts at signaling decreases in process variability. When combining the lower-sided HHW1 chart with the upper-sided HHW2 chart, the combined HHW-C chart can detect overall changes in process variability more effectively than the two-sided CH, SJ, HHW1, and HHW2 charts. Unlike the CH and SJ charts which may have different values of the Z-ARL's and S-ARL's at any value of process variability, the proposed HHW1, HHW2 and HHW-C charts, due to the ad hoc construction, all have the same Z-ARL's and S-ARL's at any value of process variability. Contrary to the result of Shu and Jiang (2008) that an EWMA chart based on the random quantity with a higher SN ratio will give better sensitivity for detecting increases in process variability, it is demonstrated in this paper that the detection performance of an EWMA chart for monitoring general changes in process variability has no connection with the SN ratio of the random quantity used. For monitoring increases in process variability, our proposed HHW2 chart can provide better design than the SJ chart. However, the standard deviation of the run length distribution associated with an ARL$_0$ should be taken into account when we use the control chart with optimal parameters to monitor the process.

**Table 5**
The optimal parameters of the SJ and HHW2 charts based on the sample size of $n = 5$ and 15.

| $n = 5$ | Z-ARL$_0$ = 100 | | Z-ARL$_0$ = 200 | | Z-ARL$_0$ = 500 | | Z-ARL$_0$ = 1000 | |
|---|---|---|---|---|---|---|---|---|
| $\sigma/\sigma_0$ | SJ | HHW2 | SJ | HHW2 | SJ | HHW2 | SJ | HHW2 |
| 1.1 | | | | | | | | |
| $(\lambda, L)$ | (0.03, 0.785) | (0.01, 0.884) | (0.03, 1.270) | (0.01, 1.209) | (0.03, 1.766) | (0.01, 1.650) | (0.03, 2.096) | (0.01, 1.996) |
| Z-ARL$_{min}$ | 19.48 | 10.43 | 29.89 | 16.00 | 47.86 | 27.58 | 64.20 | 40.33 |
| 1.2 | | | | | | | | |
| $(\lambda, L)$ | (0.03, 0.785) | (0.01, 0.884) | (0.03, 1.270) | (0.01, 1.209) | (0.04, 1.917) | (0.01, 1.650) | (0.04, 2.235) | (0.01, 1.996) |
| Z-ARL$_{min}$ | 9.66 | 4.58 | 13.91 | 6.33 | 20.11 | 9.86 | 24.77 | 13.54 |
| 1.3 | | | | | | | | |
| $(\lambda, L)$ | (0.03, 0.785) | (0.01, 0.884) | (0.11, 1.989) | (0.01, 1.209) | (0.12, 2.454) | (0.01, 1.650) | (0.10, 2.658) | (0.01, 1.996) |
| Z-ARL$_{min}$ | 6.40 | 2.95 | 9.06 | 3.81 | 11.86 | 5.51 | 14.08 | 7.23 |
| 1.4 | | | | | | | | |
| $(\lambda, L)$ | (0.03, 0.785) | (0.01, 0.884) | (0.20, 2.27) | (0.01, 1.209) | (0.16, 2.476) | (0.01, 1.650) | (0.14, 2.795) | (0.01, 1.996) |
| Z-ARL$_{min}$ | 4.84 | 2.24 | 6.37 | 2.77 | 8.04 | 3.77 | 9.37 | 4.77 |
| 1.5 | | | | | | | | |
| $(\lambda, L)$ | (0.03, 0.785) | (0.01, 0.884) | (0.37, 2.502) | (0.01, 1.209) | (0.27, 2.766) | (0.01, 1.650) | (0.21, 2.941) | (0.01, 1.996) |
| Z-ARL$_{min}$ | 3.93 | 1.86 | 4.80 | 2.22 | 5.95 | 2.88 | 6.84 | 3.55 |
| 1.6 | | | | | | | | |
| $(\lambda, L)$ | (0.49, 2.294) | (0.01, 0.884) | (0.48, 2.573) | (0.01, 1.209) | (0.38, 2.859) | (0.01, 1.650) | (0.33, 3.066) | (0.01, 1.996) |
| Z-ARL$_{min}$ | 3.21 | 1.63 | 3.80 | 1.89 | 4.65 | 2.36 | 5.31 | 2.82 |
| 1.7 | | | | | | | | |
| $(\lambda, L)$ | (0.56, 2.334) | (0.01, 0.884) | (0.55, 2.604) | (0.01, 1.209) | (0.52, 2.915) | (0.01, 1.650) | (0.43, 3.113) | (0.01, 1.996) |
| Z-ARL$_{min}$ | 2.70 | 1.48 | 3.14 | 1.67 | 3.78 | 2.02 | 4.29 | 2.38 |
| 2.0 | | | | | | | | |
| $(\lambda, L)$ | (0.68, 2.385) | (0.01, 0.884) | (0.67, 2.642) | (0.01, 1.209) | (0.67, 2.940) | (0.01, 1.650) | (0.64, 3.140) | (0.01, 1.996) |
| Z-ARL$_{min}$ | 1.89 | 1.24 | 2.10 | 1.34 | 2.41 | 1.52 | 2.66 | 1.69 |
| $n = 15$ | Z-ARL$_0$ = 100 | | Z-ARL$_0$ = 200 | | Z-ARL$_0$ = 500 | | Z-ARL$_0$ = 1000 | |
| $\sigma/\sigma_0$ | SJ | HHW2 | SJ | HHW2 | SJ | HHW2 | SJ | HHW2 |
| 1.1 | | | | | | | | |
| $(\lambda, L)$ | (0.03, 1.012) | (0.01, 0.875) | (0.03, 1.463) | (0.01, 1.202) | (0.04, 2.175) | (0.01, 1.656) | (0.04, 2.529) | (0.01, 1.995) |
| Z-ARL$_{min}$ | 10.61 | 4.53 | 15.27 | 6.38 | 21.91 | 10.11 | 27.08 | 13.98 |
| 1.2 | | | | | | | | |
| $(\lambda, L)$ | (0.03, 1.012) | (0.01, 0.875) | (0.18, 2.506) | (0.01, 1.202) | (0.14, 2.843) | (0.01, 1.656) | (0.13, 3.125) | (0.01, 1.995) |
| Z-ARL$_{min}$ | 5.04 | 2.11 | 6.56 | 2.66 | 8.30 | 3.70 | 9.69 | 4.72 |
| 1.3 | | | | | | | | |
| $(\lambda, L)$ | (0.36, 2.477) | (0.01, 0.875) | (0.35, 2.828) | (0.01, 1.202) | (0.26, 3.134) | (0.01, 1.656) | (0.24, 3.401) | (0.01, 1.995) |
| Z-ARL$_{min}$ | 3.21 | 1.51 | 3.82 | 1.75 | 4.66 | 2.23 | 5.31 | 2.69 |
| 1.4 | | | | | | | | |
| $(\lambda, L)$ | (0.50, 2.629) | (0.01, 0.875) | (0.48, 2.957) | (0.01, 1.202) | (0.42, 3.319) | (0.01, 1.656) | (0.37, 3.562) | (0.01, 1.995) |
| Z-ARL$_{min}$ | 2.27 | 1.26 | 2.62 | 1.39 | 3.11 | 1.65 | 3.50 | 1.91 |
| 1.5 | | | | | | | | |
| $(\lambda, L)$ | (0.63, 2.723) | (0.01, 0.875) | (0.62, 3.048) | (0.01, 1.202) | (0.57, 3.413) | (0.01, 1.656) | (0.53, 3.663) | (0.01, 1.995) |
| Z-ARL$_{min}$ | 1.77 | 1.14 | 1.99 | 1.22 | 2.30 | 1.37 | 2.56 | 1.54 |
| 1.6 | | | | | | | | |
| $(\lambda, L)$ | (0.70, 2.758) | (0.01, 0.875) | (0.69, 3.080) | (0.01, 1.202) | (0.66, 3.451) | (0.01, 1.656) | (0.63, 3.703) | (0.01, 1.995) |
| Z-ARL$_{min}$ | 1.48 | 1.08 | 1.62 | 1.13 | 1.83 | 1.23 | 2.00 | 1.33 |
| 1.7 | | | | | | | | |
| $(\lambda, L)$ | (0.75, 2.781) | (0.01, 0.875) | (0.77, 3.112) | (0.01, 1.202) | (0.72, 3.473) | (0.01, 1.656) | (0.71, 3.728) | (0.01, 1.995) |
| Z-ARL$_{min}$ | 1.31 | 1.05 | 1.40 | 1.08 | 1.54 | 1.14 | 1.66 | 1.20 |
| 2.0 | | | | | | | | |
| $(\lambda, L)$ | (0.92, 2.828) | (0.01, 0.875) | (0.90, 3.145) | (0.01, 1.202) | (0.87, 3.512) | (0.01, 1.656) | (0.85, 3.763) | (0.01, 1.995) |
| Z-ARL$_{min}$ | 1.08 | 1.01 | 1.11 | 1.02 | 1.16 | 1.03 | 1.20 | 1.05 |

**Table 6**
The zero-state ARL's for the SJ chart when $(\lambda, L) = (0.001, 0.0345)$ and $n = 5$.

| $\sigma/\sigma_0$ | Z-ARL | s.e. |
|---|---|---|
| 1.0 | 199.71 | 1.85 |
| 1.1 | 6.73 | 0.02 |
| 1.2 | 3.52 | 0.01 |
| 1.3 | 2.48 | 0.01 |
| 1.4 | 2.00 | 0.00 |
| 1.5 | 1.72 | 0.00 |
| 1.6 | 1.54 | 0.00 |
| 1.7 | 1.42 | 0.00 |
| 1.8 | 1.33 | 0.00 |
| 1.9 | 1.27 | 0.00 |
| 2.0 | 1.22 | 0.00 |

## References


Acosta-Mejia, C.A., Pignatiello Jr., J.J., 2000. Monitoring process dispersion without subgrouping. Journal of Quality Technology 32, 89–102.

Acosta-Mejia, C.A., Pignatiello Jr., J.J., Rao, B.V., 1999. A comparison of control charting procedures for monitoring process dispersion. IIE Transactions 31, 569–579.

Barr, D.R., Sherrill, E.T., 1999. Mean and variance of truncated normal distributions. The American Statistician 53, 357–361.

Box, G.E.P., 1954. Some theorems on quadratic forms applied in the study of analysis of variance problems: effect of inequality of variance in one-way classification. Annals of Mathematical Statistics 25, 290–302.

Box, G.E.P., Hunter, W., Hunter, J., 1978. Statistics for Experiments. John Wiley & Sons, New York, NY.

Castagliola, P., 2005. A new $S^2$-EWMA control chart for monitoring the process variance. Quality and Reliability Engineering International 21, 781–794.

Castagliola, P., Celano, G., Fichera, S., Giuffrida, F., 2007. A variable sampling interval $S^2$-EWMA control chart for monitoring the process variance. International Journal of Technology Management 37, 125–146.

Chang, T.C., Gan, F.F., 1995. A cumulative sum control chart for monitoring process variance. Journal of Quality Technology 27, 109–119.

Chen, A., Chen, Y.K., 2007. Design of EWMA and CUSUM control charts subject to random shift sizes and quality impacts. IIE Transactions 39, 1127–1141.

Chen, G.M., Cheng, S.W., Xie, H.S., 2001. Monitoring process mean and variability with one EWMA chart. Journal of Quality Technology 33, 223–233.

Crowder, S.V., Hamilton, M., 1992a. Average run lengths of EWMA controls for monitoring a process standard deviation. Journal of Quality Technology 24, 44–50.

Crowder, S.V., Hamilton, M., 1992b. An EWMA for monitoring a process standard deviation. Journal of Quality Technology 24, 12–21.

Hawkins, D.M., 1981. A CUSUM for a scale parameter. Journal of Quality Technology 13, 228–231.

Human, S.W., Chakraborti, S., Smit, C.F., 2010. Shewhart-type control charts for variation in phase I data analysis. Computational Statistics and Data Analysis 54, 863–874.

Jandhyala, V.K., Fotopoulos, S.B., Hawkins, D.M., 2002. Detection and estimation of abrupt changes in the variability of a process. Computational Statistics and Data Analysis 40, 1–19.

Knoth, S., 2006. Computation of the ARL for CUSUM-$S^2$ Schemes. Computational Statistics and Data Analysis 51, 499–512.

Lawless, J.F., 2003. Statistical Models and Methods for Lifetime Data, 2nd ed.. John Wiley & Sons, New York, NY.

Liu, J.Y., Xie, M., Goh, T.N., Chan, L.Y., 2007. A study of EWMA chart with transformed exponential data. International Journal of Production Research 45, 743–763.

Lowry, C.A., Champ, C.W., Woodall, W.H., 1993. The performance of control charts for monitoring process variation. Communication in Statistics 21, 409–437.

Lucas, J.M., Saccucci, M.S., 1990. Exponentially weighted moving average control schemes: properties and enhancements. Technometrics 32, 1–12.

Machado, M.A.G., Costa, A.F.B., 2008. The double sampling and the EWMA charts based on the sample variances. International Journal of Production Economics 114, 134–148.

Maravelakis, P.E., Castagliola, P., 2009. An EWMA chart for monitoring the process standard deviation when parameters are estimated. Computational Statistics and Data Analysis 53, 2653–2664.

Montgomery, D.C., 2008. Introduction to Statistical Quality Control, 6th ed.. John Wiley, Hoboken, NJ.

Ng, C.H., Case, K.E., 1989. Development and evaluation of control charts using exponentially weighted moving averages. Journal of Quality Technology 21, 242–250.

Page, E.S., 1954. Continuous inspection schemes. Biometrika 42, 243–254.

Page, E.S., 1963. Controlling the standard deviation by CUSUM and warning lines. Technometrics 5, 307–315.

Quesenberry, C.P., 1995. On properties of Q charts for variables. Journal of Quality Technology 27, 184–203.

Renolds Jr., M.R., Stoumbos, Z.G., 2006. Comparisons of some exponentially weighted moving average control charts for monitoring the process Mean and variance. Technometrics 48, 550–567.

Riaz, M., 2008. A dispersion control chart. Communication in Statistics: Simulation and Computation 37, 1239–1261.

Roberts, S.W., 1959. Control chart tests based on geometric moving averages. Technometrics 1, 239–250.

Shu, L.J., Jiang, W., Wu, S.J., 2007. A one-sided EWMA control chart for monitoring process means. Communication in Statistics: Simulation and Computation 36, 901–920.

Shu, L.J., Jiang, W., 2008. A new EWMA chart for monitoring process dispersion. Journal of Quality Technology 40, 319–331.

Sparks, R., 2003. Monitoring for increases in process variance. Australian and New Zealand Journal of Statistics 45, 383–394.

Sweet, A.L., 1986. Control charts using coupled exponentially weighted moving averages. IIE Transactions 18, 26–33.

Tuprah, K., Ncube, M., 1987. A comparison of dispersion quality control charts. Sequential Analysis 6 (2), 155–163.

Vermaat, M.B., Does, R.J.M.M., Bisgaard, S., 2008. EWMA control chart limits for first- and second-order autoregressive processes. Quality and Reliability Engineering International 24, 573–584.

Wortham, A.W., Ringer, L.J., 1971. Control via exponential smoothing. Transportation and Logistic Review 7, 33–39.

Zhang, J., Zou, C., Wang, Z., 2010. A control chart based on likelihood ratio test for monitoring process mean and variability. Quality and Reliability Engineering International 26, 63–73.

Zhou, Q., Luo, Y., Wang, Z., 2010. A control chart based on likelihood ratio test for detecting patterned mean and variance shifts. Computational Statistics and Data Analysis 54, 1634–1645.